

Calculated spin and orbital moments in the surfaces of the 3d metals Fe, Co, and Ni and their overlayers on Cu(001)

O. Hjortstam and J. Trygg

Condensed Matter Theory Group, Department of Physics, University of Uppsala, Box 530, Uppsala, Sweden

J. M. Wills

Theoretical Division, Los Alamos National Laboratory, Los Alamos, New Mexico 87545

B. Johansson and O. Eriksson

Condensed Matter Theory Group, Department of Physics, University of Uppsala, Box 530, Uppsala, Sweden

(Received 16 March 1995; revised manuscript received 13 July 1995)

The spin and orbital moments of the surfaces of Fe, Co, and Ni as well as of overlayers of these metals deposited on Cu have been calculated using a full-potential linear muffin-tin orbital method in a slab geometry. With one exception, Ni on Cu(001), the calculated spin moments are considerably enhanced at the surface, which is in agreement with previous theoretical and experimental work for some of the presently studied systems. We argue that the Ni- d -Cu- d hybridization is responsible for the reduced Ni spin moment in the case of a Ni monolayer on a Cu(001) substrate. The orbital moment is enhanced at the surface for all of the studied cases, sometimes by as much as a factor of 2 relative to the value found in the bulk. Based on our theoretical calculations we propose that an experimental confirmation of an enhanced orbital magnetic moment on a surface is most likely to be found for a monolayer of Co on a Cu(001) substrate or for the Fe(001) surface layer. Experimental work on Co on Cu(001) confirm this behavior.

I. INTRODUCTION

During the last decades it has become possible to prepare and measure the magnetism of clean surfaces in ultrahigh vacuum and a number of interesting observations have been made. Developments of theoretical models which treat surfaces have also been quite successful. Of central interest to the present investigation is the fact that the spin moment on surfaces is very often (but not always) enhanced relative to its value in the bulk material. There have been a number of theoretical investigations addressing this behavior. For instance, from theoretical work the spin moments of the surface of Fe, Co, and Ni are known to be enhanced.¹⁻¹² Most of the attention has been focused on the magnetism in 3d materials, although the possibility to observe magnetism in 4d and 5d elements in a surface geometry has been suggested.¹³⁻¹⁹ A simple explanation for the tendency towards enhanced magnetic moments at the surface is that the coordination number is lowered at the surface and therefore the width of the d band is reduced. Most often this effect is dominating and as a result the spin moment is enhanced.

The situation is much less clear concerning the orbital moment and little work has been done to extract this quantity. On general grounds one might expect that also this property should be enhanced at the surface due to at least three effects.⁹ First, at the surface the d bands become more narrow, causing larger spin moments. The net orbital moment is composed of a spin-up and a spin-down electron contribution, each with a different sign. If one spin band is filled, the orbital moment associated to this band is zero. Thus a large spin moment, which saturates one spin band and has a non-negligible occupation of the other spin band, enhances the orbital moment. Second, the symmetry is reduced at the sur-

face and from this point of view the crystal field quenching of the orbital moment is expected to be reduced, resulting in an enhanced surface orbital moment. Third, the value of the density of states (DOS) at the Fermi level, E_F , is larger than in the bulk. Previously it was shown that a large DOS at E_F results in an enhanced orbital moment.²⁰ A number of theoretical investigations^{5,9,11,12} have indeed shown that the orbital moment of the surface atoms of Fe, Co, and Ni is enhanced compared to the bulk and present magnetic circular dichroism (MCD) measurements on thin Co films²¹ have shown a quantitative enhancement of the orbital moment for thin Co films. Earlier MCD measurements have also indicated some enhancement of the orbital moment for Ni surfaces²² and Co/Pd interfaces.²³

The present investigation has partly been motivated by the fact that recently experimental work has been performed on Co and Ni overlayers on an fcc Cu substrate.^{21,24} By means of magnetic circular dichroism (MCD) experiments, spin and orbital moments were extracted for systems with varying overlayer thickness. The study of Ref. 21 also included a low coverage of Co on fcc Cu(001) and this particular system is addressed theoretically in the present report. For thin monolayers of Co on fcc Cu(001) it was demonstrated that the ratio between the orbital and spin moments is enhanced compared to the ratio found for bulk Co. The conclusion from this experiment is thus that there is an enhancement of the spin and orbital moments at the surface. MCD measurements for a Ni overlayer on a Cu(001) substrate showed that the Ni moment was constant for systems with 2-6 layers of Ni. Unfortunately this study gave less information for one monolayer of Ni on Cu(001), which is what we have studied here. The experimental findings mentioned above have motivated

us to undertake the present theoretical investigation of these materials.

Since the present paper concerns magnetism of Fe, Co, and Ni in surface geometries we like to mention that during the last decade a large number of reports on this subject have been published.^{1–12,21–32}

II. DETAILS OF THE CALCULATIONS

The calculational method presently used³³ is based on a slab technique, as done previously by others,^{34–38} in combination with linear muffin-tin orbitals.³⁹ The details of the technique will be presented elsewhere³³ and here we only give the main features of our theory. In short the approach is quite similar to the method published in Ref. 38. No approximation is made concerning the shape of the density or potential, and this so-called full potential treatment is quite important when considering surface geometries. In order to achieve this we adopt a base geometry based on muffin-tin spheres, an interstitial region, and a vacuum region. Inside the muffin-tin spheres and in the interstitial region our expansion of the density, potential, and wave function is essentially identical to our full-potential bulk code.⁴⁰ Thus, inside the muffin tins the density and potential are expanded by means of spherical harmonic functions times a radial component. In the interstitial region the expansion of the density and potential makes use of a Fourier series. The interstitial basis function is a Bloch sum of Neuman and Hankel functions. Each Neuman or Hankel function is then augmented (replaced) by a numerical basis function inside the muffin-tin spheres, in the standard way of the linear muffin-tin orbital method.³⁹ Since a Bloch sum of atomic centered Hankel or Neuman functions is an object which has the periodicity of the underlying lattice one may expand it in a Fourier series, something which we have done. Evaluating matrix elements of the Hamiltonian and overlap from the interstitial region thus involves relatively simple analytical functions: plane waves. In the vacuum region the basis function is composed of plane waves parallel to the surface times a numerical function which depends only on the z direction (perpendicular to the surface). The z -dependent part of the vacuum basis function is a solution to the Schrödinger equation for a planar averaged potential. The continuity and differentiability of the wave function at the boundary between the vacuum and the interstitial is ensured by requiring that each parallel component of the wave function in the vacuum region match to the corresponding component in the interstitial.³³ To put things simply, the vacuum region may be seen as an extra sphere, with infinite radius, since the Neuman or Hankel functions which come from the interstitial region are augmented (replaced) by numerical functions in the vacuum region (just as is done inside the spheres). The vacuum region is typically chosen to extend some 10–20 a.u. outside the surface boundary and at this distance we impose a boundary condition of the z -dependent part of the vacuum wave function, namely that it should equal the analytical solution for a planar, constant potential.

Furthermore, the calculations are all-electron as well as fully relativistic. The latter is obtained by including the mass velocity and Darwin terms (and higher order terms) in the calculation of the radial functions (inside the muffin-tin

spheres) whereas the spin-orbit coupling was included at each variational step using an (ℓ, s) basis. Moreover, the present calculations made use of a so-called double basis, to ensure a well-converged wave function. This means that we used two Hankel or Neuman functions each attaching to its own radial function with an (n, l) quantum number. We thus had two $4s$, two $4p$, and two $3d$ orbitals in our expansion of the crystal-slab wave function. We note here that even though we have made use of plane waves in the Fourier expansion of the wave function in the interstitial region, the matrix size is not larger than $36 \cdot n \times 36 \cdot n$, in our calculations, where n is the number of atoms per cell (the size would be $18 \cdot n \times 18 \cdot n$ if we had made use of a single-basis set, remember that the matrix size is doubled due to the spin-orbit coupling).

The direction of the moment is chosen to be perpendicular to the surface and we thus neglect the possibility that the easy axis might be in another direction. Note that one has to be especially careful about the symmetry in these calculations since, due to the spin-orbit coupling, spin has a specific orientation in space. Thus one has to consider the magnetic group of the crystal, as for example is done by Cracknell.⁴¹ In Ref. 41 it is shown that although it is true that certain elements of the magnetic group are products of a rotation (or rotation followed by space inversion) and the time reversal operator (anti-unitary elements), the space inversion followed by a 180° rotation around the z axis (z reflection) is a unitary element for the bcc, fcc, and hcp slabs. We have thus treated atoms at positions (x, y, z) and $(x, y, -z)$ as equivalent and this means that we only have four inequivalent atom types in our seven-layer thick slabs. We did not include the antiunitary elements of the magnetic group in these calculations and have thus performed calculations of slightly lower symmetry than what is needed. Although this does not introduce errors in the description of the symmetry properties of our slabs we have performed calculations for an object with slightly to low symmetry.

Further, the calculations were converged using ≥ 64 k points in the two-dimensional Brillouin zone and the number of k points were increased until the calculated moments were stabilized within 3%. The sampling of the Brillouin zone was done over the irreducible two-dimensional wedge which was $1/4$ for the cubic materials and $1/3$ for the hexagonal ones (these numbers would be $1/8$ and $1/6$, for the cubic and hexagonal systems, respectively, if antiunitary elements are considered). In all calculations we have used a seven-atomic-layer-thick slab (except for the calculations of free standing monolayers). In order to investigate if the slab thickness is sufficiently large, to ensure that the central layer is bulklike, we checked that the magnetic moment, the occupation numbers, and the density of states (DOS) for the middle layer compare well with data from bulk calculations. Since we make use of different expansions of the density in the three different regions there may be (small) differences of the charge density at the boundary between the interstitial and the muffin-tin sphere as well as between the interstitial and the vacuum. This difference can of course be made to vanish simply by increasing the number of functions used in the expansion of the density in a certain region, for instance the number of plane waves used in the Fourier series in the expansion of the interstitial charge. Typically, in our calcula-

TABLE I. Calculated spin and orbital moments (in μ_B), including the spin-orbit coupling but not the orbital polarization, inside the MT sphere for the different atomic layers for Fe, Co, and Ni seven-layer slabs. S denotes the surface layer while the central layer is denoted by C and the subsurface layer by $S-1$ and so forth.

Layer	Fe			Co			Ni		
	M_S	M_L	M_L/M_S	M_S	M_L	M_L/M_S	M_S	M_L	M_L/M_S
S	2.94	0.096	0.033	1.79	0.090	0.050	0.73	0.062	0.085
$S-1$	2.33	0.054	0.023	1.68	0.079	0.047	0.61	0.049	0.080
$S-2$	2.38	0.047	0.020	1.62	0.075	0.046	0.61	0.043	0.070
C	2.25	0.049	0.022	1.63	0.075	0.046	0.59	0.042	0.071
Interstitial	0.16			-0.26			-0.19		

tions, the discontinuities at the boundaries between the muffin-tin sphere and the interstitial region as well as at the boundaries between the interstitial region and the vacuum region is not larger than 0.1% of the density at these points. Furthermore, the calculations were based on the local spin density approximation (LSDA) with the von Barth–Hedin parametrization. In our calculations we also included an orbital polarization correction suggested by Eriksson *et al.*,⁴² which has the form $\Delta E_{\ell,\sigma,m_\ell} = -R_{\ell,\sigma} L_\sigma m_\ell$. Where $\Delta E_{\ell,\sigma,m_\ell}$ is added to the diagonal elements of the Hamiltonian matrix. The Racah parameter, $R_{\ell,\sigma}$ (usually called B for d states), was calculated self-consistently using the radial d wave functions for each spin channel. L_σ is the orbital moment for the σ -spin channel and m_ℓ is the magnetic quantum number.

III. RESULTS

A. Fe, Co, and Ni surfaces

Using the above-mentioned full-potential linear muffin-tin orbital method we have performed electronic structure calculations for bcc Fe(001) ($a=5.42$ a.u.), hcp Co(0001) ($a=4.74$ a.u. and $c/a=1.62$), and fcc Ni(001) ($a=6.82$ a.u.) slabs. The calculated spin and orbital moments for each layer are presented in Tables I and II and in Fig. 1. The numbers listed in Table I were obtained by neglecting the orbital polarization term whereas the numbers in Table II included the effect of the orbital polarization. The moments of a specific layer are taken to be the moments inside the muffin-tin sphere for the corresponding atom (neglecting the interstitial moment). In Tables I and II we also present the spin moment contribution from the interstitial region. In principle there is

also an orbital contribution to the magnetism in this region but this moment is very small and was neglected. The total moment of the slab is the sum of the moments (spin and orbital) from each layer, the moment from the interstitial region, and the moment from the vacuum region (which is very small). We note here that both the spin and orbital moments in Tables I and II (as well as in the results to be described below) are dominated by the d orbitals. As seen from Tables I and II the spin moment for all layers (surface as well as bulk) decrease when traversing the series (i.e., the moments follow the so called Slater-Pauling curve). This behavior is known to originate from band filling effects. In order to illustrate this we show the density of states (DOS) projected on the different muffin-tin spheres of the various atomic layers (Fig. 2). In Fig. 2 it is seen that the majority-spin band is almost filled for all layers and elements (in bulk Fe the majority-spin band is not quite as filled as it is in Co and Ni, see below). Since Co has one more, and Ni two more, valence electrons than Fe the minority-spin band becomes more filled when the series is traversed (since the majority-spin band is almost saturated), and the spin moment therefore decreases. Moreover, the spin moment is enhanced for the surface layer for all three systems (Fig. 1 and Tables I and II). The enhancement of the spin moment is 31% for Fe, 10% for Co, and 26% for Ni. In absolute values the enhancement of the moment of the surface atoms is $\sim 0.69\mu_B$ for Fe, $\sim 0.16\mu_B$ for Co, and $0.15\mu_B$ for Ni. This is in good agreement with previous theoretical findings.^{1–12} The reason for the enhanced spin moment on the surface is that the bandwidth of the surface atoms is smaller than the corresponding bandwidth of the bulk atoms (central layer, C), due to the reduced coordination number (i.e., the lower number of nearest neighbors). As pointed out above the sur-

TABLE II. Calculated spin and orbital moments (in μ_B), including the spin-orbit coupling as well as the orbital polarization, inside the MT sphere for the different atomic layers for Fe, Co, and Ni seven-layer slabs. The same notation as in Table I is used.

Layer	Fe			Co			Ni		
	M_S	M_L	M_L/M_S	M_S	M_L	M_L/M_S	M_S	M_L	M_L/M_S
S	2.94	0.184	0.063	1.79	0.158	0.088	0.73	0.093	0.127
$S-1$	2.33	0.096	0.041	1.68	0.129	0.077	0.61	0.067	0.110
$S-2$	2.38	0.077	0.032	1.62	0.123	0.076	0.61	0.058	0.095
C	2.25	0.082	0.036	1.63	0.123	0.075	0.58	0.058	0.100
Interstitial	0.16			-0.26			-0.19		

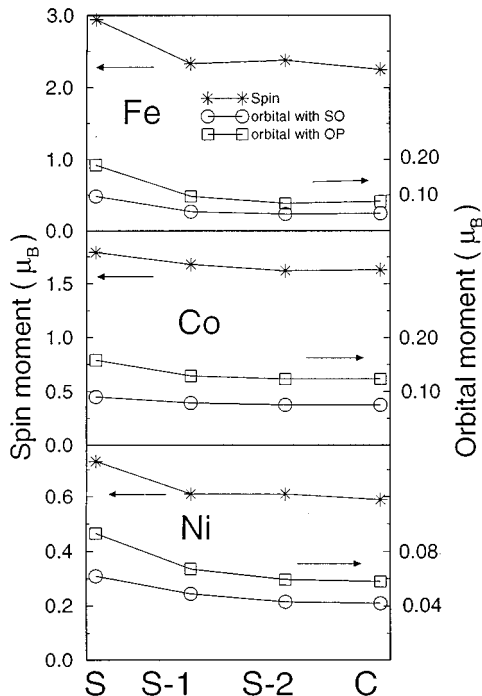


FIG. 1. Calculated spin and orbital moments for Fe, Co, and Ni seven-layer slabs. The scale on the left side shows the values for the spin moment while the right scale shows the orbital moment values. The spin moments are marked by asterisks. The squares show the calculated orbital moment when both spin-orbit interaction and orbital polarization is used while the circles show the calculated orbital moment when only the spin-orbit interaction is used.

face moment of Fe is more enhanced than for Co and Ni. The reason for this can be seen in Fig. 2. Namely, bcc Fe has a majority-spin band which is less saturated than the corresponding band in Co and Ni. A narrowing of the band at the surface will therefore result in a larger increase of the moment for Fe compared to Co and Ni. In Fig. 1 we demonstrate the spin profile when we are penetrating these materials from the surface to the bulk. We observe that for Fe(001) there are small oscillations in the spin moment. These Friedel-like oscillations have earlier been found in bcc Fe by means of similar theoretical calculations.^{3,12} However these oscillations have very small amplitude and bulk spin moments are found after only 3–4 layers. For Co and Ni we do not see this oscillatory behavior.

From Tables I and II and Fig. 1 we note that the orbital moments are strongly enhanced at the surface. In the calculations which include the orbital polarization the enhancement is 120% for Fe, 30% for Co, and 60% for Ni. This enhancement originates partly from the enhanced spin moment, as discussed above. However, there are additional reasons for enhanced orbital moments at surfaces. The lack of a large orbital moment in transition metals is traditionally explained as due to a large crystal field quenching of the orbital moment. However, for the surface atoms the local symmetry is lowered and the crystal field quenching of the orbital moment is therefore less effective. This results in an enhanced orbital moment at the surface. The reason for why the orbital moment in Co is relatively less enhanced than in Fe and Ni (Fig. 1) can also be understood using these arguments since

Co has a lower symmetry already in the bulk (and therefore a larger bulk orbital moment) and the relative lowering of the symmetry at the surface is therefore not as pronounced. The validity of these arguments can be inspected from the DOS of for instance bcc Fe (Fig. 2) where the bulk DOS shows the characteristic two-peak feature which originates from the crystal field splitting of a d level into e_g and t_{2g} states. This splitting is reduced at the surface of Fe (since the two-peak structure is absent), revealing a reduced crystal field quenching of the orbital moment at the surface. This was also pointed out in Ref. 9. A third effect which tends to enhance the orbital moment for the surface atoms was pointed out in Refs. 20 and 43. There it was argued that the orbital moment will to some extent depend on the value of the DOS at E_F ; a large DOS at E_F should result in a large orbital moment. An inspection of the value of the DOS at E_F for the different atomic layers and the different metals (Fig. 2) shows that the DOS is normally enhanced at the surface (since the bands normally are narrower at the surface). Figure 2 shows that the strongest enhancement of the DOS at E_F is found for bcc Fe and according to the arguments presented in Refs. 20 and 43, this is consistent with the fact that the enhancement of the orbital moment is largest for this surface (Tables I and II and Fig. 1). In Fig. 1 we show that also the orbital moment takes its “bulk value” only a few atomic layers below the surface. Also for this property we have found small oscillation in Fe(001) when penetrating the material from the surface to the bulk.

We now compare our calculated spin and orbital moments, and especially their ratio, with other theoretical data as well as with experiment. If we compare our calculated orbital moments obtained when not treating the orbital polarization (Table I) we find good agreement with the previous surface studies; in most cases within 10–20 % of the data of Bruno,⁵ Eriksson *et al.*,⁹ and Wu *et al.*¹² Our calculated orbital moments (using orbital polarization, Table II) are ~ 40 to ~ 90 % larger than the orbital moments calculated by Bruno,⁵ Eriksson *et al.*,⁹ and Wu *et al.*¹² On the other hand, our bulk moments (central layer) compare well with the bulk calculation of Söderlind *et al.*⁴⁴ as well as with experiment.⁴⁵ This result demonstrates the importance of the orbital polarization correction used in the present investigation. Wu *et al.*¹² calculated the ratio between the orbital and spin moments in the center of a seven-layer thick slab and found it to be 0.024, 0.042, and 0.081 for Fe, Co, and Ni, respectively. These numbers may be compared to bulk MCD measurements, listed by Carra *et al.*,⁴⁶ which give an experimental value of this ratio of 0.067, 0.065, and 0.095 for Fe, Co and Ni, respectively. However, later MCD measurements,⁴⁷ for Fe and Co, give the ratios 0.044 and 0.096, respectively. Also, experimental data for the $\langle l_z \rangle / \langle s_z \rangle$ ratio, deduced from measurements of the g factor (using the de Haas–van Alphen technique), published by Bonnenberg *et al.*,⁴⁵ give the ratios 0.044, 0.097, and 0.098 μ_B for bulk Fe, Co, and Ni, respectively. When we compare our calculated ratios for the central layers (including the orbital polarization) in Table II with experiment we observe that the agreement between the presently calculated bulk data and experiment^{47,45} is fair, and it is clear that at least part of the difference between the previous theory^{5,9,11,12} and experiment is due to the neglect of the orbital polarization.

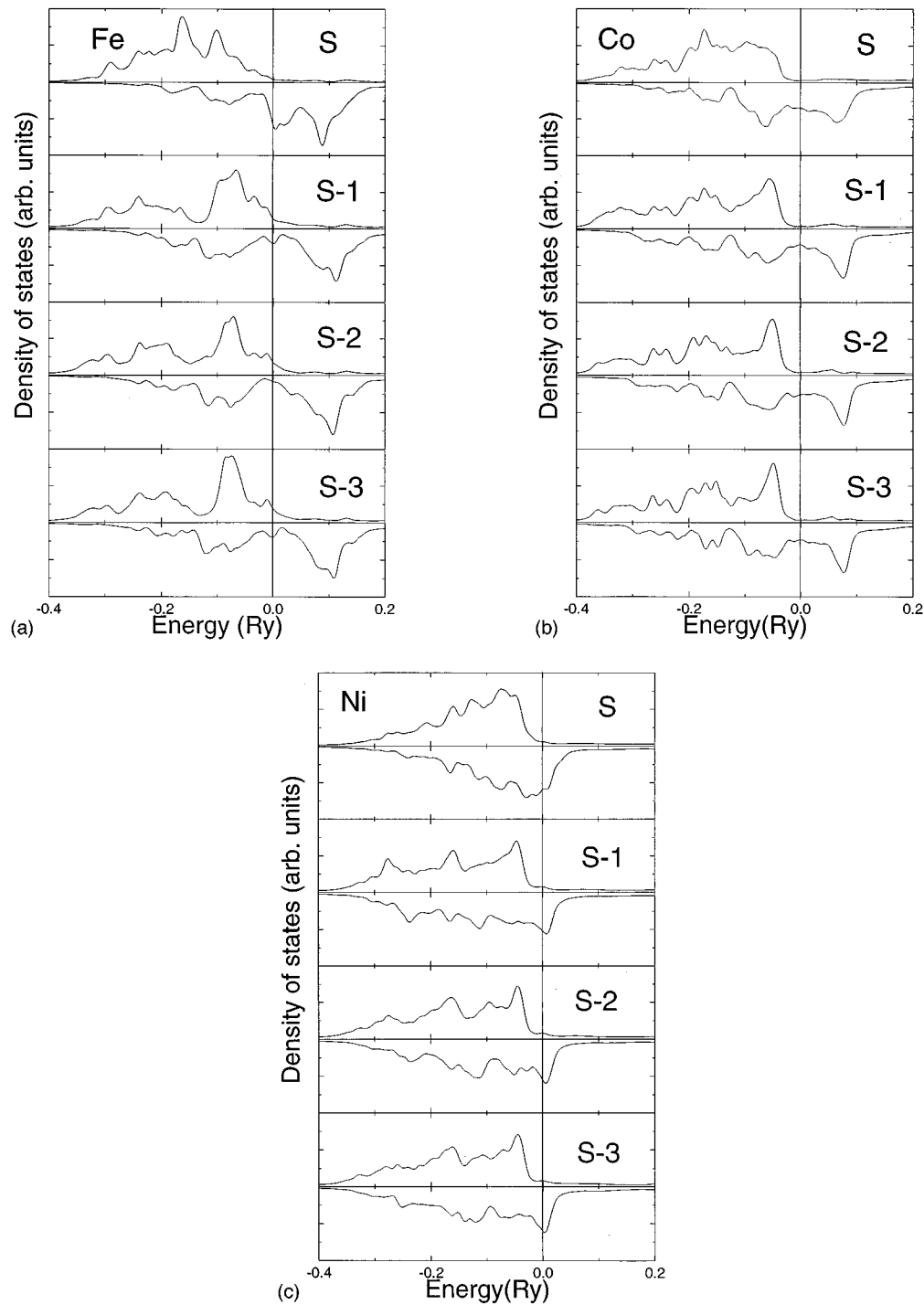


FIG. 2. Calculated layer- and spin-projected density of states for seven-atomic-layer-thick slabs of (a) Fe bcc(001), (b) Co hcp(0001), and (c) Ni fcc(001). S denotes the surface layer while the central layer is denoted by C and the subsurface layer by $S-1$ and so forth. The upper panel for each layer shows the DOS for the majority spin while the lower panel shows the minority spin DOS.

For completeness we also present our calculated work functions for the Fe, Co, and Ni surfaces, and they are 4.8 eV, 5.2 eV, and 5.7 eV, respectively. This is in good agreement with other calculated values and experiment.^{2-4,6,9,10,48}

B. Fe, Co, and Ni overlayers on Cu(001)

We have also carried out electronic structure calculations for an overlayer of Fe, Co, and Ni on a fcc Cu(001) sub-

strate. The overlayer (one atomic layer) is assumed to have the same crystal structure and lattice constant ($a=6.82$ a.u.) as the Cu(001) substrate. The calculated spin and orbital moments for each layer are presented in Tables III and IV. In Table III we show results obtained when neglecting the orbital polarization whereas in Table IV we present results from calculations treating the orbital polarization. The DOS projected to the overlayer atoms is shown in Fig. 3. The major part of the interstitial contribution to the spin moment

TABLE III. Calculated spin and orbital moments (in μ_B), including the spin-orbit coupling but not the orbital polarization, inside the MT sphere for the different atomic layers for Fe/5Cu/Fe, Co/5Cu/Co, and Ni/5Cu/Ni seven-layer slabs. The same notation as in Table I is used.

Layer	Fe/5Cu/Fe			Co/5Cu/Co			Ni/5Cu/Ni		
	M_S	M_L	M_L/M_S	M_S	M_L	M_L/M_S	M_S	M_L	M_L/M_S
<i>S</i>	2.81	0.071	0.025	1.85	0.121	0.065	0.45	0.055	0.122
<i>S</i> -1	0.05			0.03			0.01		
<i>S</i> -2	-0.01			-0.01			~ 0		
<i>C</i>	~ 0			~ 0			~ 0		
Interstitial	0.11			-0.06			-0.02		

comes from the region close to the overlayer atoms. For the overlayer of Fe and Co on Cu the spin and orbital moments are enhanced compared to the corresponding values in the bulk material. The reason for the enhanced spin and orbital moments in these two systems is the same as discussed above for the metal surfaces. However, for the Ni overlayer the spin moment is decreased to a value of $0.45 \mu_B$ (compared to $\sim 0.6 \mu_B$ for the bulk spin moment of Ni) whereas the orbital moment is increased compared to the bulk value. This unexpected behavior of the spin moment will be discussed in detail in Sec. III D below. Concerning orbital magnetism we note that the orbital moment of the Co overlayer is much larger than for the Fe and Ni overlayers. The reason for this is at least partially found in the DOS plot (Fig. 3) where it is clear that the DOS at E_F for the minority-spin band is larger in Co on Cu(001). A similar behavior, with a large DOS at E_F , is found for Ni, but in this case the increase of the orbital moment is not as pronounced because of the reduced spin moment in this system. However, as a consequence of the large peak at E_F the M_L/M_S ratio is relatively large for Ni on Cu(001).

Let us now compare our theoretical results (Table IV) with the MCD measurement in Ref. 21. Experimentally it was observed that the ratio between the orbital and spin moments for a monolayer of Co on Cu (fcc) is enhanced compared to the bulk ratio. From Table IV we extract the calculated ratio to be 0.141 for the Co overlayer on Cu which is in fair agreement with the experimental ratio 0.19. Notice that the experimental ratio is obtained from an extrapolation of Co films which are ≥ 3 atomic layers thick, a procedure which may introduce a small uncertainty.

The work functions for the Fe, Co, and Ni monolayers on Cu(001) are calculated to be 5.9 eV, 5.3 eV, and 5.1 eV, respectively. This is in good agreement with other theoretical results.^{26,28,29}

C. Fe, Co, and Ni free standing monolayers

In order to compare with the overlayer calculations we have also calculated the electronic structure for a free standing monolayer of Fe, Co, and Ni with the same lattice geometry and interatomic spacing as for the overlayers in the previous section. Such calculations are not entirely of a hypothetical nature since it has been demonstrated that epitaxial growth of for instance Fe on MgO yields a surface magnetism which is almost “two dimensional,” i.e., which in many ways behaves as a free standing monolayer.⁴⁹ The present analysis may be viewed as a precursor for such a more realistic study. The spin and orbital moments from the monolayer calculations are presented in Tables V (spin-orbit) and VI (spin-orbit and orbital polarization). In the case of free standing monolayers we notice that both the spin and orbital moments are enhanced compared to both the overlayer calculations as well as to the metal surfaces. However it is interesting that the enhancement of the spin moment is not as strong as the enhancement of the orbital moment. The reason for this is that these systems have almost saturated spin moments. As a result the spin moments of the monolayers (Tables V and VI) are enhanced with $\sim 5\text{--}35\%$ compared to the data in Tables I–IV (not comparing with Ni on Cu). The orbital moment of the monolayers is enhanced considerably more, sometimes by over a factor of 2. The strong enhancement of the orbital moment is partly an effect of the increased spin moment as well as the increased value of the DOS at E_F . However, these two effects alone cannot explain the trend of the orbital moments in Tables V and VI since the orbital moment (which has a maximum for Co) does not follow the trend of the spin moment (strictly decreasing when the series is traversed) nor the trend of the DOS at E_F (not shown) and it appears that the monolayer calcula-

TABLE IV. Calculated spin and orbital moments (in μ_B), including the spin-orbit coupling as well as the orbital polarization, inside the MT sphere for the different atomic layers for Fe/5Cu/Fe, Co/5Cu/Co, and Ni/5Cu/Ni seven-layer slabs. The same notation as in Table I is used.

Layer	Fe/5Cu/Fe			Co/5Cu/Co			Ni/5Cu/Ni		
	M_S	M_L	M_L/M_S	M_S	M_L	M_L/M_S	M_S	M_L	M_L/M_S
<i>S</i>	2.81	0.126	0.045	1.85	0.261	0.141	0.45	0.087	0.193
<i>S</i> -1	0.05			0.03			0.01		
<i>S</i> -2	-0.01			-0.01			~ 0		
<i>C</i>	~ 0			~ 0			~ 0		
Interstitial	0.11			-0.06			-0.02		

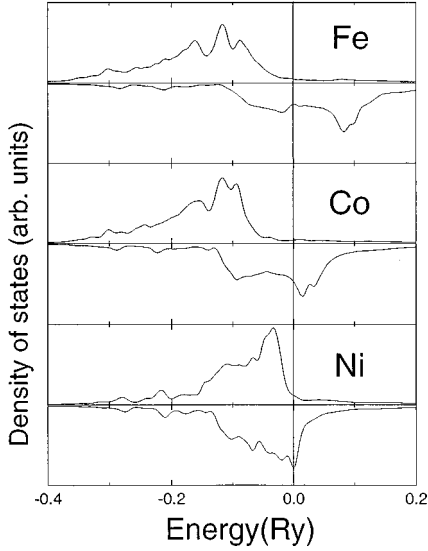


FIG. 3. Calculated layer- and spin-projected density of states for the overlayer of a seven-atomic-layer-thick slabs of Fe/5Cu/Fe, Co/5Cu/Cu, and Ni/5Cu/Ni. In all cases the geometry was fcc(001). The upper panel for each layer shows the DOS for the majority spin while the lower panel shows the minority spin DOS.

tions serve as a good example for illustrating the effect of band filling on the orbital moment. Above we have discussed several reasons for finding enhanced orbital moments; reduced symmetry, a large value of the DOS at E_F , and enhanced spin moments. For the monolayers the symmetry is the same for Fe, Co, and Ni and the spin moment is saturated and decreases therefore with $\sim 1\mu_B$ from one element to the next in the series. The trend displayed by the orbital moment, which is much larger in Co than in Fe and Ni, can therefore not be explained from symmetry arguments nor from the spin moment. Moreover, the value of the DOS at E_F is similar for the three elements and thus the trend cannot be explained from this effect either. However, as indicated above the explanation lies in the particular filling of the orbitals (band filling effect). To illustrate this we consider the extreme case of infinitesimally narrow bands, i.e., the Fe, Co, and Ni free atoms. If the $3d$ level of Fe, Co, and Ni occupies 6.5, 7.5, and 8.5 electrons, respectively, one expects orbital moments of $2.5\mu_B$, $3.0\mu_B$, and $2.5\mu_B$, respectively. This is the same trend as one finds in Tables V and VI. Due to that these atomic levels broaden into (narrow) bands in the monolayers the orbital moments are reduced considerably compared to the atomic values but the trend is the same as one expects from the atomic limit. The data in Tables V and VI therefore illustrate the importance of band filling effects on the orbital moments. Quite generally this effect tends to give

larger orbital moments for Co compared to Fe and Ni, something which very often is observed experimentally.

If one would be able to grow for instance Co on a substrate such that the electronic structure of Co maintained a two-dimensional character, Co on MgO might be a good example, one should be able to observe large orbital moments (of the magnitude listed in Table VI). As a consequence it is likely that such a material might display a large surface magnetocrystalline anisotropy, Kerr rotation angle, and other effects which are related to orbital magnetism and relativistic effects.

D. Decreased spin moment in the Ni overlayer on Cu

In this section we will return to the decrease of the spin moment of the Ni overlayer on the fcc Cu(001) substrate. This decreased Ni moment is well known from theory.^{27,29,50} However the cause of it has been a source of confusion. In Ref. 27 the spin moment for the Ni overlayer on Cu(001) was calculated to be $0.39\mu_B$ which agrees well with our result. In that paper the decrease is claimed to be due to a change in the $3d$ occupation number of the Ni overlayer atoms compared to bulk Ni as well as to the surface of Ni metal. An alternative explanation was provided in Ref. 50 where, by means of a tight-binding model, the decrease of the Ni spin moment was claimed to be an effect of strong hybridization between the Ni $3d$ electrons and the Cu s and p electrons. This difference in the explanation of the decreased Ni moment on a Cu substrate has motivated us to investigate this effect in more detail. First of all we observe that in our calculations we cannot find any significant change in the occupation number of the monolayer compared to the surface atom of Ni metal or to the Ni atom on the Cu substrate. The d occupation of the surface atoms is a little higher for the overlayer systems compared to the metal surfaces, which would suggest a decreased Ni moment on the Cu substrate. However, the difference in occupation number between the Ni overlayer and the Ni metal surface is far from sufficient to explain the large reduction in moment.

Next, we analyze the effect of hybridization for the Ni/Cu(001) system. A very useful estimate of the hybridization between states of (t, l) and (t', l') character (t stands for atom type and l stands for angular momentum) has been suggested by Andersen *et al.*⁵¹ This analysis is based on common concepts in the linear muffin-tin orbital method in the atomic sphere approximation (ASA). We now study the hybridization in the Ni/Cu(001) system by means of the method outlined in Ref. 51. First, the amount of (t, l) character present in the (t', l') band (which is a measure of the hybridization) can be estimated from the following expression:

TABLE V. Calculated spin and orbital moments (μ_B), including spin-orbit coupling but not the orbital polarization, inside the MT sphere for a free standing monolayer of Fe, Co, and Ni.

Layer	Fe			Co			Ni		
	M_S	M_L	M_L/M_S	M_S	M_L	M_L/M_S	M_S	M_L	M_L/M_S
S	2.96	0.094	0.032	2.07	0.142	0.069	0.99	0.122	0.123
Interstitial	0.06			-0.01			-0.01		

TABLE VI. Calculated spin and orbital moments (in μ_B), including the spin-orbit coupling as well as the orbital polarization, inside the MT sphere for a free standing monolayer of Fe, Co, and Ni.

Layer	Fe			M_S	Co		M_S	Ni	
	M_S	M_L	M_L/M_S		M_L	M_L/M_S		M_L	M_L/M_S
S	2.96	0.199	0.067	2.06	0.338	0.164	0.99	0.235	0.237
Interstitial	0.06			-0.01			-0.01		

$$N_{it} = \frac{\Delta_{it}\Delta_{t't'}|S_{t't'}^{it}|^2}{(C_{t't'} - C_{it})^2}. \quad (1)$$

In the equation above C_{it} is the center of the (t,l) band, Δ_{it} is a bandwidth parameter, and $|S_{t't'}^{it}|^2$ is normally referred to as the second moment of the structure constants.⁵¹ The latter quantity can be calculated in real space using the expression in Ref. 51. The hybridization between the Ni d band and the Cu s , Cu p , and Cu d bands can thus be estimated from Eq. (1) and this analysis reveals that the Ni- d -Cu- d hybridization is dominating. Next, we analyze the shifts of the Ni d bands due to the hybridization with the Cu d states. We start out by considering the Ni d states from the monolayer calculation. In this case, where of course there is no hybridization between Cu d states, the Ni d minority-spin band is centered at -0.100 Ry and the Ni d majority-spin band is centered at -0.035 Ry. The exchange splitting is thus 0.065 Ry for the monolayer. If we now consider the presence of Cu d states, which are centered at -0.180 Ry, one can estimate the shift in energy of the Ni d band due to the hybridization with the Cu d band using the expression

$$\delta E_{it} = \frac{\Delta_{it}\Delta_{t't'}|S_{t't'}^{it}|^2}{(C_{t't'} - C_{it}) \cdot n_t(2l+1)}, \quad (2)$$

where n_t is the number of atoms of type t in the unit cell. We have inserted into this equation the band positions mentioned above. A real space summation of $|S_{t't'}^{it}|^2$ gives a value of ~ 75 for this quantity and the values of Δ_{it} and $\Delta_{t't'}$ are approximately 0.015 Ry. With these values we estimate that the Ni d majority-spin band is pushed upwards an amount 0.041 Ry and the Ni d minority-spin band by an amount 0.023 Ry, due to the hybridization with the Cu d states. Therefore, as a consequence of the hybridization with the Cu d states, the exchange splitting of the Ni d band is reduced from 0.065 Ry to 0.047 Ry. An inspection of Fig. 3 shows that the fully self-consistent value of the exchange splitting of the Ni d states on the Cu substrate is very close to our estimate. Thus we conclude that the Ni- d -Cu- d hybridization is responsible for the reduced moment of the Ni atoms on the Cu substrate. The hybridization with the Cu states also tends to reduce the magnetic moments of the Fe and Co overlayers, but in this case the narrowing of the bands due to the lower coordination number is sufficient to produce large spin moments.

IV. CONCLUSIONS

In the present work we have studied the spin and orbital magnetism for the metal surfaces of Fe, Co, and Ni, monoatomic overlayers of these materials on a Cu fcc(001) sub-

strate, and single layer slabs of Fe, Co and Ni. Figure 4 shows a summary of the calculated magnetic properties, M_S, M_L , and M_L/M_S , of Fe, Co, and Ni, in the different geometries discussed here. We have found that with one exception, Ni on Cu(001), the spin moments of Fe, Co, and Ni are enhanced at the surface. The orbital moments are found to be enhanced at the surface for all systems, sometimes with more than a factor of 2 relative to the bulk value. The importance of treating orbital polarization effects^{42,52-54} is also demonstrated. The enhanced spin moments are caused by band narrowing effects at the surface due to a reduction of the coordination number. However, in the case of Ni on Cu(001) we have showed that the Cu- d -Ni- d hybridization to some extent quenches the exchange splitting, producing a spin moment which is lower than in bulk Ni metal. We argue that the enhancement of orbital magnetism is caused by one or more of the following mechanisms; enhanced spin moments, lowered symmetry at the surface, large value of DOS at E_F , and band filling effects. The observation that several effects are responsible for the surface behavior is somewhat unfortunate since it would be much simpler to predict this

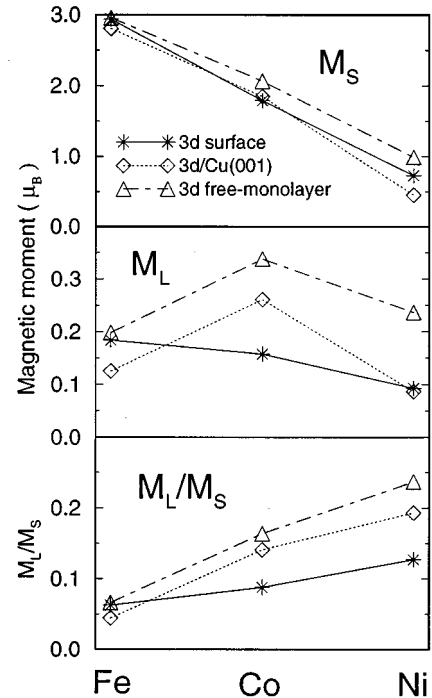


FIG. 4. Summary of calculated properties for the surface layers in different geometries for Fe, Co, and Ni. The upper panel shows the calculated spin moment (M_S), the middle panel shows the orbital moment (M_L), and the lower panel shows the ratio M_L/M_S . In all cases the orbital polarization term is used in the calculations.

surface property if one effect would dominate over the others. As it turns out one has to perform extensive calculations in order to obtain a reliable estimate of the orbital moment. Finally we have found a fair agreement for the Co/Cu(001) system concerning the calculated ratio between the orbital and spin moments and the corresponding experimental value deduced from MCD experiments.²¹ Further, both our spin and orbital moments for the central layer of Fe, Co, and Ni agree well with bulk calculations,⁴⁴ *g*-factor measurements,⁴⁵ as well as MCD measurements for Fe and Co performed by Chen *et al.*⁴⁷ The accuracy of our calculations in reproducing spin and orbital moments of bulk Fe, Co, and Ni gives support to that our theoretical method is reliable in reproducing

experimental spin and orbital moments for bulk, interface, and surface systems.

ACKNOWLEDGMENTS

Valuable discussions with D. Arvanitis are acknowledged. O.E., O.H., and B.J. are grateful to the Swedish Natural Science Research Foundation for financial support. The work forms part of a project supported by a European Community Human Capital and Mobility program. We are grateful to NSC (Swedish National Supercomputing Center), Linköping for supplying some of the computer time used in the present work. The support from the materials consortium No. 9 is appreciated.

-
- ¹D. Wang, A.J. Freeman, and H. Krakauer, *Phys. Rev. B* **26**, 1340 (1982).
- ²O. Jepsen, J. Madsen, and O.K. Andersen, *Phys. Rev. B* **26**, 2790 (1982).
- ³S. Ohnishi, A.J. Freeman, and M. Weinert, *Phys. Rev. B* **28**, 6741 (1983).
- ⁴E. Wimmer, A.J. Freeman, and H. Krakauer, *Phys. Rev. B* **30**, 3113 (1984).
- ⁵P. Bruno, *Phys. Rev. B* **39**, 865 (1989).
- ⁶Chun Li, A.J. Freeman, and C.L. Fu, *J. Magn. Magn. Mater.* **94**, 134 (1991).
- ⁷A.J. Freeman and Ruqian Wu, *J. Magn. Magn. Mater.* **100**, 497 (1991).
- ⁸A. Vega, L.C. Balbás, J. Dorantes-Dávila, and G.M. Pastor, *Surf. Sci.* **251/252**, 55 (1991).
- ⁹O. Eriksson, A.M. Boring, R.C. Albers, G.W. Fernando, and B.R. Cooper, *Phys. Rev. B* **45**, 2868 (1992).
- ¹⁰M. Aldén, S. Mirbt, H.L. Skriver, N.M. Rosengaard, and B. Johansson, *Phys. Rev. B* **46**, 6303 (1992).
- ¹¹R. Wu, D. Wang, and A.J. Freeman, *Phys. Rev. B* **71**, 3581 (1993).
- ¹²R. Wu, D. Wang, and A.J. Freeman, *J. Magn. Magn. Mater.* **132**, 103 (1994).
- ¹³O. Eriksson, R.C. Albers, and A.M. Boring, *Phys. Rev. Lett.* **66**, 1350 (1991).
- ¹⁴M. J. Zhu, D.M. Bylander, and L. Kleinman, *Phys. Rev. B* **43**, 4007 (1991).
- ¹⁵S. Blügel, *Phys. Rev. Lett.* **68**, 851 (1992).
- ¹⁶R. Wu and A.J. Freeman, *Phys. Rev. B* **45**, 7222 (1992).
- ¹⁷I. Morrison, D.M. Bylander, and L. Kleinman, *Phys. Rev. Lett.* **71**, 1083 (1993).
- ¹⁸H. Li, S.C. Wu, D. Tian, Y.S. Li, J. Quinn, and F. Jona, *Phys. Rev. Lett.* **44**, 1438 (1991).
- ¹⁹S.C. Wu, K. Garrison, A.M. Begley, F. Jona, and P.D. Johanson, *Phys. Rev. B* **49**, 14 081 (1994).
- ²⁰H. Ebert, R. Zeller, B. Drittler, and P.H. Dederichs, *J. Appl. Phys.* **67**, 4576 (1990).
- ²¹M. Tisher, O. Hjortstam, D. Arvanitis, J. Hunter Dunn, F. May, K. Baberschke, J. Trygg, J.M. Wills, B. Johansson, and O. Eriksson, *Phys. Rev. Lett.* **75**, 1602 (1995).
- ²²G. van der Laan, M.A. Hoyland, M. Surman, C.F.J. Flipse, and B.T. Thole, *Phys. Rev. Lett.* **69**, 3827 (1992).
- ²³M.G. Samant, J. Stöhr, S.S.P. Parkin, G.A. Held, B.D. Hermsmeier, F. Herman, M. van Schilfgaarde, L.-C. Duda, D.C. Mancini, N. Wassdahl, and R. Nakajima, *Phys. Rev. Lett.* **72**, 1112 (1994).
- ²⁴M. Tischer, D. Arvanitis, and T. Yokoyama, *Surf. Sci.* **306/309**, 1096 (1994).
- ²⁵C.L. Fu and A.J. Freeman, *Phys. Rev. B* **35**, 925 (1987).
- ²⁶C. Li, A.J. Freeman, and C.L. Fu, *J. Magn. Magn. Mater.* **83**, 52 (1990).
- ²⁷D. Wang, A.J. Freeman, and H. Krakauer, *Phys. Rev. B* **26**, 1340 (1982).
- ²⁸Hong Huang, Xue-yuan Zhu, and J. Hermanson, *Phys. Rev. B* **29**, 2270 (1984).
- ²⁹I. Turek, J. Kudrnovský, V. Drchal, and P. Weinberger, *Phys. Rev. B* **49**, 3352 (1994).
- ³⁰G.D. Waddill, J.G. Tobin, and D.P. Pappas, *J. Appl. Phys.* **73**, 6749 (1993).
- ³¹J.G. Tobin, G.D. Waddill, and D.P. Pappas, *Phys. Rev. Lett.* **68**, 3642 (1992).
- ³²L.H. Tjeng, Y.U. Idzerda, P. Rudolf, F. Sette, and C.T. Chen, *J. Magn. Magn. Mater.* **109**, 288 (1992).
- ³³J.M. Wills and O. Eriksson (unpublished).
- ³⁴E. Wimmer, H. Krakauer, M. Weinert, and A.J. Freeman, *Phys. Rev. B* **24**, 864 (1981).
- ³⁵O. Jepsen, J. Madsen, and O.K. Andersen, *Phys. Rev. B* **18**, 606 (1978).
- ³⁶M.J. Zhu, D.M. Bylander, and L. Kleinman, *Phys. Rev. B* **42**, 2874 (1990).
- ³⁷D.R. Hamann, *Phys. Rev. Lett.* **42**, 662 (1979); L.F. Mattheis and D.R. Hamann, *Phys. Rev. B* **33**, 823 (1986).
- ³⁸H. Krakauer and B.R. Cooper, *Phys. Rev. B* **16**, 605 (1977); C.Q. Ma, M.V. Ramana, B.R. Cooper, and H. Krakauer, *J. Vac. Sci. Technol. A* **1**, 1095 (1983); C.Q. Ma, M.V. Ramana, B.R. Cooper, and H. Krakauer, *Phys. Rev. B* **34**, 3854 (1986); G.W. Fernando, B.R. Cooper, M.V. Ramana, H. Krakauer, and C.Q. Ma, *Phys. Rev. Lett.* **56**, 2299 (1986).
- ³⁹O.K. Andersen, *Phys. Rev. B* **12**, 3060 (1975); H.L. Skriver, *The LMTO Method* (Springer, Berlin, 1984).
- ⁴⁰This method has been used in a number of applications [see, for instance, P. Söderlind, O. Eriksson, B. Johansson, J.M. Wills, and A.M. Boring, *Nature* **374**, 524 (1995)] and details of it may be found in J.M. Wills and B.R. Cooper, *Phys. Rev. B* **36**, 3809 (1987); D.L. Price and B.R. Cooper, *ibid.* **39**, 4945 (1989).
- ⁴¹A.P. Cracknell, *J. Phys. C* **2**, 1425 (1969).
- ⁴²O. Eriksson, B. Johansson, and M.S.S. Brooks, *Phys. Rev. B* **41**, 7311 (1990).

- ⁴³O. Eriksson, B. Johansson, R.C. Albers, A.M. Boring, and M.S.S. Brooks, Phys. Rev. B **42**, 2707 (1990).
- ⁴⁴P. Söderlind, O. Eriksson, B. Johansson, R.C. Albers, and A.M. Boring, Phys. Rev. B **45**, 12 911 (1992).
- ⁴⁵D. Bonnenberg, K.A. Hempel, and H.P.J. Wijn, in *Landolt-Börnstein Numerical Data and Functional Relationships in Science and Technology*, edited by H.P.J. Wijn (Springer-Verlag, Berlin, 1986), Group 3, Vol. 19.
- ⁴⁶P. Carra, B.T. Thole, M. Altarelli, and X. Wang, Phys. Rev. Lett. **70**, 694 (1993).
- ⁴⁷C.T. Chen *et al.* (private communication).
- ⁴⁸F.R. de Boer, R. Boom, W.C.M. Mattens, A.R. Miedema, and A.K. Niessen, in *Cohesion in Metals*, edited by F.R. de Boer and D.G. Pettifor (North-Holland, Amsterdam, 1988), Vol. I, p. 676.
- ⁴⁹Chun Li and A.J. Freeman, Phys. Rev. B **43**, 780 (1991).
- ⁵⁰J. Tersoff and L.M. Falicov, Phys. Rev. B **26**, 6186 (1982).
- ⁵¹O.K. Andersen, W. Klose, and H. Nohl, Phys. Rev. B **17**, 1209 (1978).
- ⁵²M.R. Norman, Phys. Rev. Lett. **64**, 1162 (1990).
- ⁵³M.R. Norman, Phys. Rev. B **44**, 1364 (1991).
- ⁵⁴L. Severin, M.S.S. Brooks, and B. Johansson, Phys. Rev. Lett. **71**, 3214 (1993).